A Bilateral Controller for Pharyngeal Swab Test Teleoperation System

Yanfeng Pu[1(✉)], Liang Li[2], Ting Wang[2], and Zhenxing Sun[2]

[1] Nanjing Customs District P. R. China, 360, Longpanzhong Road, Qinhuai District, Nanjing, China
64016663@qq.com

[2] College of Electrical Engineering and Control Science, Nanjing Tech University, Nanjing 21816, China

Abstract. Due to the novel pneumonia virus outbreak and gradual normalization, throat swab detection has become an important means for customs entry and exit personnel. However, the current detection methods make the medical staff exposed to the dangerous environment for a long time, which is very easy to cause the infection of medical staff. In view of the relative shortage of medical staff, this paper proposes to use the teleoperation system for pharyngeal swab detection, and puts forward the corresponding bilateral teleoperation controller. Finally, its feasibility is verified by numerical simulations.

Keywords: Teleoperation system · Bilateral teleoperation controller · Numerical simulation

1 Introduction

Nearly 300, 000 people worldwide died from complications caused by COVID-19 virus, and more than 4.3 million cases were infected. According to data from the Asian Development Bank (ADB), the global economic losses caused by the COVID-19 epidemic this year may be more than doubled over the period of 5 trillion and 800 billion minus 8.8 trillion dollars. Reuters reported that the ADB's estimate is equivalent to 6.4%9.7% of global GDP, worse than its April forecast. The ADB estimated in April that the global economic loss may be between $2.0 trillion and $4.1 trillion, depending on the duration time of the anti epidemic blockade measures are implemented. This new analysis shows novel coronavirus pneumonia (COVID-19) that may cause a very significant economic impact. At the same time, it also highlights that policy intervention can play an important role in helping reduce economic losses. After the health crisis caused China's economy to actually stagnate in the first quarter, the number of reported infection cases and deaths in several countries and regions increased, leading to extensive travel restrictions and home orders. The Asian Development Bank (ADB) said that the measures taken to control the spread of the epidemic may cause economic losses of US $1.7 trillion to US $2.5 trillion in Asia and US $1.1 trillion to US $1.6 trillion in China. Travel restrictions

S. Yang and H. Lu (Eds.): ISAIR 2022, CCIS 1700, pp. 112–117, 2022.
https://doi.org/10.1007/978-981-19-7946-0_10

and blockades could reduce global trade by $1.7 trillion to $2.6 trillion, resulting in the unemployment of 158 million to 242 million people [1, 2].

Novel coronavirus pneumonia test reagent, currently approved by the China CDC researcher Feng Luzhao, mainly includes two categories, one is nucleic acid detection reagent, the other is antibody detection reagent. So far, the State Food and drug administration has approved 12 nucleic acid detection reagents and 8 antibody detection reagents, including 5 kinds of colloidal gold method and 3 kinds of magnetic particle chemiluminescence method. The nucleic acid detection process includes sample processing, nucleic acid extraction, PCR detection and other steps. The average detection time takes 23 h. Since it directly detects the viral nucleic acid in the collected samples, it has strong specificity and relatively high sensitivity. It is the main detection method at present. Antibody detection includes colloidal gold method and magnetic particle chemiluminescence method. The average detection time of colloidal gold method is about 15 min. However, if the serum is used instead of whole blood, this serum treatment still needs some time. If whole blood is used, it is about 15 min. Magnetic particle chemiluminescence generally takes 3060 min. Antibody detection is to detect the antibody level in human blood. In the early stage of disease infection, there may be no antibody in human body, so it has a detection window. Therefore, antibody detection can be used for auxiliary diagnosis of cases with negative nucleic acid detection and screening of cases, but it can not replace nucleic acid detection method. With the normalization and scattered development of the epidemic situation, pharyngeal swab detection is still the most frequently used method in countries all over the world [3, 4].

In China and many other countries in the world, pharyngeal swab detections are heavily relying on medical staff which causes the shortage of medical staffs owing to the close contact. In addition, it also aggravates the infection risk of medical staff although medical staffs wear protective clothing. Therefore, in this paper, we introduce of using teleoperation system to achieve accurate and fast pharyngeal swab test. In the pharyngeal swab test teleoperation system, the medical staff operates the master haptic manipulator to make the slave manipulator to lamp the cotton swab and to realize pharyngeal swab sampling. In this case, medical staffs may located at the place far from the person to be sampled.

The rest of the paper is organized into the following 4 sections. Section 2 analyzes the dynamic equation of pharyngeal swab test teleoperation system. Section 3 describes the bilateral sliding mode control method. Section 4 performs the numerical simulation and discusses results. Conclusions are discussed in the Conclusions section.

2 Dynamic Equation of Pharyngeal Swab Test Teleoperation System

Assuming both the master and the slave manipulators apply the same two degree of freedom (2-DOF) manipulator with two links and three joints, the dynamic equation of the pharyngeal swab test teleoperation system can be expressed as follows:

$$M_i(q_i)\ddot{q}_i + C_i(q_i, \dot{q}_i)\dot{q}_i + G_i(q_i) = \tau_i + d_i,\ \mathrm{i} = \mathrm{m}, \mathrm{s} \tag{1}$$

where, Subscribes m and s are respectively represented the master side and the slave side. $q_i \in R^n$ is the rotation angle vector of three joints of both the master and the slave manipulators. $\dot{q}_i \in R^n$ and $\ddot{q}_i \in R^n$ are angular velocity and angular accelerations of the master and the slave manipulators in the joint space. $d_i \in R^n$ is the lump disturbances involving the model uncertainties and external disturbances and has the upper boundedness. $M_i(q_i) \in R^{n\times n}$ are the inertia matrix of the master and the slave sides. $C_i(q_i, \dot{q}_i) \in R^{n\times n}$ are the combination of centrifugal force and Coriolis force matrix of the master and the slave sides. $G_i(q_i) \in R^{n\times n}$ are the gravitational matrix of the master and the slave sides. $\tau_i \in R^n$ are respectively torque vectors of the master and the slave manipulators. The teleoperation dynamic equation satisfied following properties.

1. The inertia matrix $M_i(q_i)$ are symmetric and positive definite. Its norm is bounded:

$$M_i(q_i) = M_i(q_i)^T > 0 \tag{2}$$

$$M_i(q_i)_{\min} \le \|M_i(q_i)\| \le M_i(q_i)_{\max} \tag{3}$$

2. $\dot{M}_i(q_i) - 2C_i(q_i, \dot{q}_i)$ are skew-symmetric matrix and it satisfies:

$$\left[\dot{M}_i(q_i) - 2C_i(q_i, \dot{q}_i)\right]^T = -\left[\dot{M}_i(q_i) - 2C_i(q_i, \dot{q}_i)\right] \tag{4}$$

3. The 2-norm of $M_i(q_i)$ is bounded with an upper limit ζ and it satisfies:

$$\forall q_i \in D_i q_i, \left\|\dot{M}_i(q_i)\right\| \le \zeta_i \tag{5}$$

3 Bilateral Teleoperation Control of Pharyngeal Swab Test Teleoperation System

In order to get high accuracy of the pharyngeal swab test, the disturbance observer is designed as follows.

$$\begin{cases} \dot{z}_i = L_i(q_i)\left(C_i(q_i, \dot{q}_i)\dot{q}_i + G_i(q_i) - \tau_i - \hat{\tau}_{di}\right) \\ \hat{\tau}_{di} = z_i + p_i(\dot{q}_i) \end{cases} i = m, s \tag{6}$$

$$L_i(q_i) = X_i^{-1} M_i^{-1}(q_i)\, i = m, s \tag{7}$$

$$p_i(q_i) = X_i^{-1}\dot{q}_i\, i = m, s \tag{8}$$

where X_i are an invertible matrix, $M_i(q_i) = M_i(q_i)^T > 0$, $i = m,s$.

The lumped disturbance and uncertainties is estimated by $\hat{\tau}_{di}$. Then, based on the disturbance observer, the bilateral controller is designed as follows.

Define the error as follows:

$$\tilde{q}_i(t) = q_i(t) - q_{di}(t) \tag{9}$$

where $\tilde{q}_i$ is tracking error and q_{di} are the desired trajectories of manipulators. Then define the auxiliary variable q_{ri} as:

$$\begin{aligned} \dot{q}_{ri} &= \dot{q}_{di} - \Lambda_i \tilde{q}_i \\ \ddot{q}_{ri} &= \ddot{q}_{di} - \Lambda_i \dot{\tilde{q}}_i \end{aligned} \tag{10}$$

where $\dot{q}_{di}$ and $\ddot{q}_{di}$ are the velocity and acceleration of the desired trajectories respectively and $\Lambda_i = diag(\lambda_{1i} \cdots \lambda_{ni})$, $\lambda_i > 0$. The control law are designed as

$$s_i = \dot{\tilde{q}}_i + \Lambda_i \tilde{q}_i \tag{11}$$

$$\tau_i = M_i(q_i)\ddot{q}_{ri} + C_i(q_i, \dot{q}_i)\dot{q}_{ri} + G_i(q_i) - K_{di}s_i - \eta_i \text{sgn}s_i - \hat{\tau}_{di} \tag{12}$$

where $K_{di} = diag(K_{d1} \cdots K_{dn})$, $K_{di} > 0$, $\eta_i \geq \max(|d_{1i}|, |d_{2i}|)$, and $\text{sgn}s_i$ is a symbolic function.

Proof: Lyapunov function V_i is considered as follows

$$V_i = \frac{1}{2} s_i^T M_i(q_i) s_i + V_{1i} \tag{13}$$

$$\begin{aligned} \dot{V}_i &= s_i^T M_i(q_i)\dot{s}_i + \frac{1}{2} s_i^T \dot{M}_i(q_i) s_i + \dot{V}_{1i} \\ &= s_i^T (u_i - C_i(q_i, \dot{q}_i)\dot{q}_i - G_i(q_i) - M_i(q_i)\ddot{q}_{ri}) + \frac{1}{2} s_i^T \dot{M}_i(q_i) s_i + \dot{V}_{1i} \\ &= -s_i^T K_{di} s_i - \eta_i \|s_i\| + \frac{1}{2} s_i^T \left(\dot{M}_i(q_i) - 2C_i(q_i, \dot{q}_i)\right) s_i + \dot{V}_{1i} \text{ From above, when } \dot{V} \equiv 0, \text{ It} \\ &= -s_i^T K_{di} s_i - \eta_i \|s_i\| + \dot{V}_{1i} \leq 0 \end{aligned}$$

It is easily seen that $s_i \equiv 0$, $\tilde{q}_i \equiv 0$. Depending on the theory of LaSalle, the teleoperation system is asymptotically stable using the above controller. As $t \to \infty$, s_i and $\tilde{q}_i$ converge exponentially to zero. That is, the teleoperation system may accomplish accurate trajectory tracking.

4 Numerical Simulations

In numerical simulations, parameters are set as the same as [5]. The observed initial value of the disturbance td is taken as [0, 0]. Other parameters are set as follows, $\Upsilon_m = \Upsilon_s = \begin{bmatrix} 0.5 & 0 \\ 0 & 0.6 \end{bmatrix}$, $X_m = X_s = \begin{bmatrix} 0.3 & 0 \\ 0 & 0.4 \end{bmatrix}$, $K_{dm} = K_{ds} = \begin{bmatrix} 100 & 0 \\ 0 & 100 \end{bmatrix}$, $\Lambda_m = \Lambda_s = \begin{bmatrix} 150 & 0 \\ 0 & 150 \end{bmatrix}$. After numerical simulations, results are illustrated as follows. Trajectory tracking of the master and the salve side are displayed respectively in Fig. 1 and Fig. 2. From results of numerical simulations, the teleoperation system may accomplish precise trajectory tracking due to the bilateral teleoperation controller.

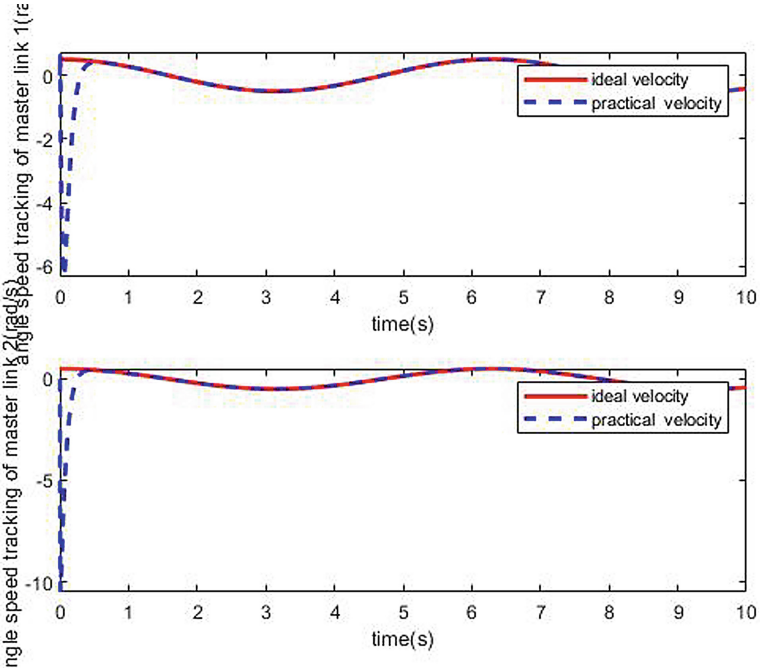

Fig. 1. Trajectory tracking of the master manipulator.

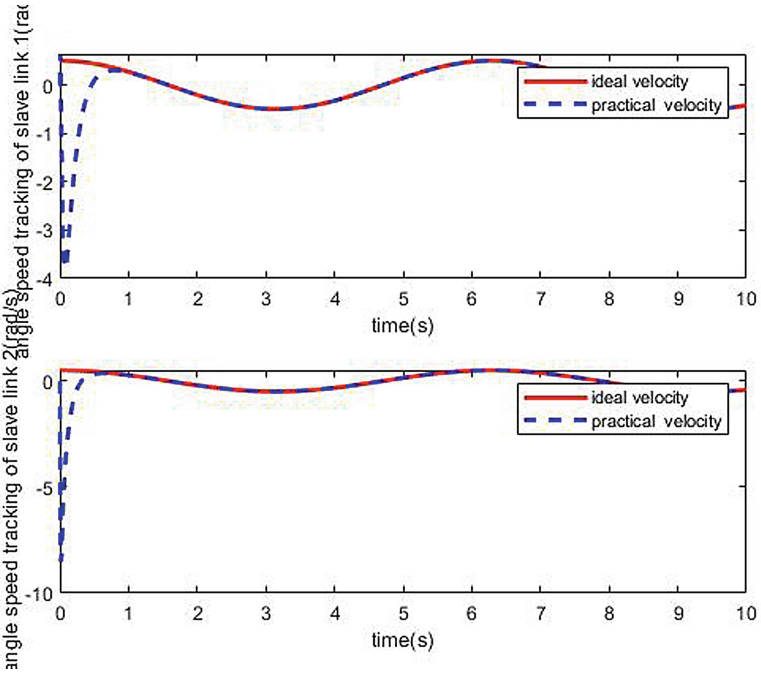

Fig. 2. Trajectory tracking of the slave manipulator.

5 Conclusion

In the paper, a teleoperation system is used to achieve accurate and fast pharyngeal swab test avoiding the infection risk of medical staff. Both of the master and the slave side take 2 DOF manipulators. A bilateral teleoperation controller is proposed for accurate trajectory tracking. The stability is analyzed and numerical simulations are performed to verify the proposed method. Results show the efficiency of the tracking performances.

Acknowledgements. This work was supported by the National Natural Science Foundation of China [grant numbers No. 61906086].

References

1. Hase, R., Kurita, T., Muranaka, E., et al.: A case of imported COVID-19 diagnosed byPCR-positive lower respiratory specimen but with PCR-negative throat swabs.Taylor& Francis, pp. 1–4 (2020). https://doi.org/10.1080/23744235.2020.1744711
2. Huang, K., Sun, Y., Chen, B., et al.: New COVID-19 saliva-based test: how good is it compared with the current nasopharyngealor throat swab test? J. Chin. Med. Assoc. **83**(10), 891 (2020). https://doi.org/10.1097/JCMA.0000000000000396
3. Vlek, A.L.M., Wesselius, T.S., Achterberg, R., Thijsen, S.F.T.: Combined throat/nasal swab sampling for SARS-CoV-2 is equivalent to nasopharyngeal sampling. Eur. J. Clin. Microbiol. Infect. Dis. **40**(1), 193–195 (2020). https://doi.org/10.1007/s10096-020-03972-y
4. Bertalan, G., Klein, C., Schreyer, S., et al.: Biomechanical properties of the hypoxic and dying brain quantified by magnetic resonance elastography. Acta Biomater. **101**, 395–402 (2020)
5. Wang, T., Li, Y., Zhang, J., Zhang, Y.: A novel bilateral impedance controls for underwater tele-operation systems **91**, 106194 (2020)
6. Huimin, L., Zhang, M., Xu, X.:Deep fuzzy hashing network for efficient image retrieval. IEEE Trans. Fuzzy Syst. **29**(1), 166176 (2020). https://doi.org/10.1109/TFUZZ.2020.2984991
7. Huimin, L., Li, Y., Chen, M., et al.: Brain intelligence: go beyond artificial intelligence. Mobile Networks Appl. **23**, 368–375 (2018)
8. Huimin, L., Li, Y., Shenglin, M., et al.: Motor anomaly detection for unmanned aerial vehicles using reinforcement learning. IEEE Internet Things J. **5**(4), 2315–2322 (2018)
9. Huimin, L., Qin, M., Zhang, F., et al.: RSCNN: A CNN-based method to enhance low-light remote-sensing images. Remote Sensing **13**(1), 62 (2020)